Available online at www.sciencedirect.com
ScienceDirect
Journal of Hazardous Materials 149 (2007) 134–143
Journal of Hazardous Materials
www.elsevier.com/locate/jhazmat

Equilibrium, kinetic and thermodynamic studies on the adsorption of *m*-cresol onto micro- and mesoporous carbon

L. John Kennedy [a], J. Judith Vijaya [b], G. Sekaran [a,*], K. Kayalvizhi [a]

[a] *Department of Environmental Technology, Central Leather Research Institute, Adyar, Chennai, Tamil Nadu, India*
[b] *Department of Chemistry, Loyola Institute of Frontier Energy, Loyola College, Chennai, Tamil Nadu, India*

Received 19 December 2006; received in revised form 22 March 2007; accepted 22 March 2007
Available online 25 March 2007

Abstract

Investigations were conducted in batch mode to study the adsorption behaviour of *m*-cresol on a porous carbon prepared from rice husk (RHAC) by varying the parameters such as agitation time, *m*-cresol concentration (50–300 mg/l), pH (2.5–10) and temperature (293–323 K). Studies showed that the adsorption decreased with increase in pH and temperature. The isotherm data were fitted to Langmuir, Freundlich, and Dubinin–Radushkevic (D–R) models. The kinetic models such as pseudo-first-order, pseudo-second-order and intraparticle diffusion models were selected to understand the reaction pathways and mechanism of adsorption process. The thermodynamic equilibrium coefficients obtained at different temperatures were used to evaluate the thermodynamic constants ΔG°, ΔH° and ΔS°. The sorption process was found to be exothermic in nature (ΔH°: −23.46 to −25.40 kJ/mol) with a decrease in entropy (ΔS°: −19.44 to −35.87 J/(mol K)). The negative value of Gibbs free energy, ΔG° indicates that the adsorption occurs via a spontaneous process. The decrease in the value of $-\Delta G^\circ$ from 17.70 to 13.54 kJ/mol with increase in pH and temperature indicates that the adsorption of *m*-cresol onto activated carbon is less favourable at higher temperature and pH range. The influence of mesopore and a possible mechanism of adsorption is also suggested.

Keywords: Adsorption; Rice husk; Equilibrium; Kinetic; Thermodynamics

1. Introduction

Substituted phenolic compounds are considered to be one of the major pollutants in wastewater as they are used as raw materials in many chemical industries. The presence of such non-biodegradable compounds in effluent discharges is of increasing concern due to the mounting evidence of adverse ecologic and public health's impacts. Therefore, removal or destruction of these substituted phenols from the effluents becomes more essential. *m*-Cresol, one of the substituted phenol is used in many industries such as production of modified phenolic resins, metal degreasing, wood preservative, ore flotation, photographic developers, paint brush cleaners, dyes, plastics, additive to lubricating oils, insecticides and antioxidants [1]. Despite of such wide applications, *m*-cresol is highly corrosive and is fatal if indigested or absorbed through skin. Hence, proper treatment of *m*-cresol by any methods is highly essential before discharging into the environment. Among the different technologies available such as aerobic, anaerobic biodegradation, chemical oxidation, ion exchange and solvent extraction, the adsorption by activated carbon has gained wide acceptance as it can, not only remove selective organic compounds up to the satisfactory limits but also can remove a broad spectrum of other inorganic and organic compounds generally discharged from any industries [2]. However, their use is limited by their high cost. This has led many workers to search for cheaper substitutes from agricultural wastes such as bagasse pith, sawdust, maize cop, coconut husk fibers, rice husk, fruit kernels and nutshells that appear to be more economically attractive in producing activated carbons [3,4]. Although rice husk-based activated carbon have been used for the removal of dyes, metal ions and phenolic compounds [5–14] as shown in Table 1, there is still lack of works on the adsorption equilibrium, kinetics and thermodynamics of *m*-cresol onto rice husk-based activated carbon (RHAC). Therefore, we focused our study to

* Corresponding author. Tel.: +91 44 24410232.
E-mail addresses: jklsac14@yahoo.co.in (L.J. Kennedy), ganesansekaran@hotmail.com (G. Sekaran).

0304-3894/$ – see front matter © 2007 Elsevier B.V. All rights reserved.
doi:10.1016/j.jhazmat.2007.03.061

Table 1
Rice husk-based porous carbon employed for adsorption in the literatures

Sl. no.	Activation	Surface area (m^2/g) (BET)	Adsorption of	Reference
1	Only carbonization/no activation	44	Chlorinated hydrocarbon	[5]
2	KOH	2000–3500	Hexavalent chromium	[6]
	NaOH	2000–3000		
3	Steam	272.5	Acid yellow 36	[7]
4	NaOH/KOH	2721/1930	Malachite green, iodine, hydroquinone, catechol, resorcin, rhodamine B	[8–11]
5	Only carbonization/no activation	–	Hexavalent chromium	[12]
6	H_3PO_4	–	Malachite green	[13]
7	HNO_3	14	2,4-Dichlorophenol	[14]
8	H_3PO_4	438.9	*m*-Cresol	Present work

prepare porous carbon from rice husk by two-stage process using H_3PO_4 activation and employ it for the adsorption of *m*-cresol.

The aim of the presents study was to investigate the *m*-cresol adsorption characteristics of RHAC taking into account equilibrium, kinetic, and thermodynamic aspects. The most commonly used isotherms such as Langmuir, Freundlich, and Dubinin–Radushkevich (D–R) equations were applied to describe and predict the adsorption equilibrium. Three simplified kinetic models including pseudo-first-order equation, pseudo-second-order equation and intraparticle diffusion models were used to determine the mechanism of adsorption. The thermodynamic parameters such as standard free energy, enthalpy, and entropy were also evaluated. The role of mesopore in influencing micropore coverage in the adsorption process and a possible mechanism is also elucidated.

2. Materials and methods

2.1. Preparation of porous carbons

Rice husk, the precursor material obtained from the agro industry was washed with water several times for the removal of dust and dried at 383 K for 6 h. The dried samples were then sieved to about 600 μm in size and this fraction was used for the preparation of carbons. The porous carbon used in this study was prepared according to our previous reports [15]. Briefly, the porous carbons were prepared in two sequential steps: precarbonization and chemical activation. In the precarbonization process the rice husk was heated at 673 K for about 4 h under nitrogen atmosphere and cooled down to room temperature at the same rate. The resulting material is labeled as precarbonized carbon (PCC). The precarbonized carbon is then subjected to chemical activation. In chemical activation process 50 g of the precarbonized carbon was agitated with 250 g of aqueous solution containing 85% H_3PO_4 by weight. The ratio of chemical activating agent/precarbonized carbon was homogeneously mixed at 358 K for 4 h. After mixing, the precarbonized carbon slurry was dried under vacuum at 383 K for 24 h. The resulted samples were then activated under nitrogen atmosphere at three different temperatures, 973, 1073 and 1173 K and maintained at the final temperature for 1 h before cooling. After cooling, the activated carbon was washed successively, several times with hot water until the pH becomes neutral and finally with cold water to remove the excess phosphorus compounds. The washed samples were dried at 383 K to get the final product. The samples heated at activation temperatures 973, 1073 and 1173 K were labeled as C700, C800 and C900.

2.2. Carbon characterization

The N_2 adsorption–desorption isotherms of RHAC were measured using an automatic adsorption instrument (Quantachrome Corp. Nova-1000 gas sorption analyzer) for the determination of surface area and total pore volumes. Prior to measurement, carbon samples were degassed at 423 K overnight. The surface area of the activated carbons was calculated using BET equation, which is the most widely used model for determining the specific surface area (m^2/g). In addition, the *t*-plot method [15] was applied to calculate the micropore volume and external surface area (mesoporous surface area). The total pore volume was estimated as liquid volume of adsorbate adsorbed at a relative pressure of 0.99. All surface area measurements were calculated from the nitrogen adsorption isotherms by assuming the area of the nitrogen molecule to be 0.162 nm^2.

The carbon, hydrogen and nitrogen content of the different heat-treated carbons were determined using CHNS 1108 model Carlo-Erba analyzer. Perkin-Elmer infrared spectrometer was used for the determination of the surface functional groups. The carbon samples were mixed with KBr of spectroscopic grade and made in the form of pellets at pressure of about 1 MPa. The pellets were about 10 mm in diameter and 1 mm thickness. The samples were scanned in the spectral range 4000–400 cm^{-1}.

2.3. m-Cresol adsorption procedure

The characteristics of the micro- and mesoporous carbon prepared from rice husk are shown in Table 2. The activated carbon C900, that possessed comparatively highest surface area 438.9 m^2/g was selected for the adsorption studies. The high surface area of C900 can be attributed to the release of certain volatile components from the work generated by acid treatment on the precursor material containing the organic and inorganic matter at the activation temperature of 900 °C. Adsorp-

Table 2
Characteristics of micro-/mesoporous carbons derived from rice husk

Sl. no.	Parameters	Sample code		
		C700	C800	C900
1	S_{BET} (m^2/g)	344.7	379.4	438.9
2	S_{mic} (m^2/g)	202.7	214.6	214.9
3	S_{meso} (m^2/g)	142.0	164.8	224.0
4	Micropore volume, V_{micro} (cm^3/g)	0.11	0.12	0.12
5	Mesopore volume, V_{meso} (cm^3/g)	0.22	0.25	0.27
6	Total pore volume, V_{tot} (cm^3/g)	0.33	0.37	0.39
7	V_{meso}/V_{tot} (%)	66.66	67.56	69.23
8	Average pore diameter (Å)	38.82	39.36	35.28
9	Production yield of carbon (%)	40.66	39.19	37.69
10	Carbon (%)	42.56	41.58	37.96
11	Hydrogen (%)	3.14	2.85	2.40
12	Nitrogen (%)	0.82	0.75	0.50
13	Moisture (%)	12.24	13.22	13.56
14	Ash (%)	41.24	41.60	45.58
15	Decolorizing power (mg/g)	67.23	68.98	69.32
16	Point of zero charge (PZC)	6.6	6.9	7.1
17	Apparent density (g/cm^3)	0.65	0.61	0.56

S_{BET}: BET surface area; S_{mic}: micropore surface area; S_{meso}: mesopore surface area.

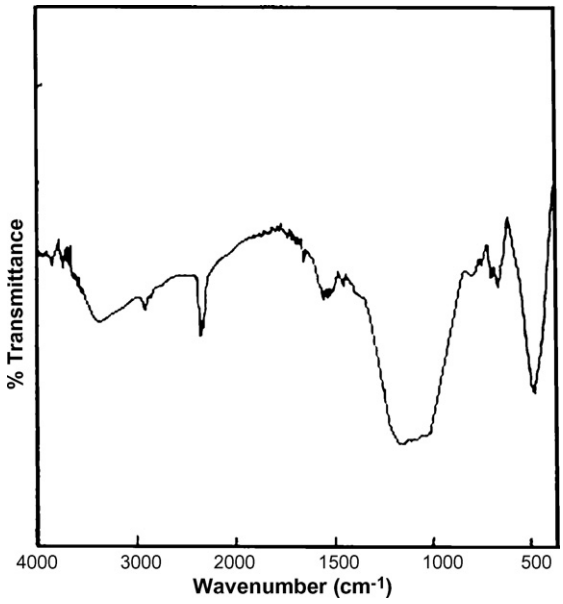

Fig. 1. FTIR spectrum of RHAC-C900 carbon derived from rice husk.

tion kinetics and equilibrium studies were conducted using batch mode adsorption technique by placing a known quantity of the adsorbent in glass bottles containing 10 ml of an aqueous solution of predetermined concentration. The adsorbent dose was 0.15 g/10 ml solution. The solutions were agitated at 100 rpm until the equilibrium is reached at a given particular temperature, pH and concentration, as agitation beyond 100 rpm had very little effect on the adsorption process. The adsorption of *m*-cresol on RHAC-C900 activated carbon from aqueous solutions were carried out at four different concentrations 50, 100, 200, 300 mg/l; pH 2.5, 5.0, 7.5, 10.0 and at four different temperatures 293, 303, 313 and 323 K in order to attain equilibrium and thus efficient adsorption. The concentration of *m*-cresol was determined during the adsorption process by Shimadzu UV–vis spectrophotometer at its wavelength of 272 nm. The amount of *m*-cresol adsorbed onto the adsorbate q_e (mg/g) were calculated according to

$$q_e = \frac{(C_0 - C_e)V}{W} \quad (1)$$

where V is the volume of the solution, C_0 the initial concentration (mg/l), C_e the equilibrium concentration (mg/l), and W is the weight of the adsorbent (g).

3. Results and discussion

3.1. FTIR spectra

The infrared spectroscopy that provides information on the chemical structure of C900 is shown in Fig. 1. The activated carbon showed a wide band at about 3350–3425 cm^{-1} that can be assigned to the O–H stretching mode of hexagonal groups and adsorbed water. The position and asymmetry of this band at lower wave numbers indicate the presence of strong hydrogen bonds [16]. A weak band at 3780–3786 cm^{-1} may be assigned to isolated O–H group. An absorption band due to aliphatic C–H at 2920 cm^{-1} is also found. A very small peak near 1700 cm^{-1} is assigned to C=O stretching vibrations of ketones, aldehydes, lactones or carboxyl groups. The weak intensity of this peak indicate that the activated carbon contain a small amount of carboxyl group. The broad peak shouldered at about 1115 cm^{-1} and a sharp peak at 805 and 475 cm^{-1} in the activated carbon sample indicate the presence of silica [15] that is one of the main composition of the rice husk derived activated carbon.

3.2. Effect of time

The effect of time for the adsorption process is carried out in order to reach the equilibrium point. The study was carried out for the given four different temperatures, pH and concentration. It was found in all set of experiments that the adsorption was rapid up to 15 min and thereafter reached equilibrium at around 75 min as shown in Fig. 2. Hence, for further kinetic studies an equilibrium time of 75 min was selected. However, the shape of the curves of *m*-cresol adsorption is almost found to be the same. The amount of *m*-cresol adsorbed (mg/g) increased with increase in agitation time and the curves for *m*-cresol with

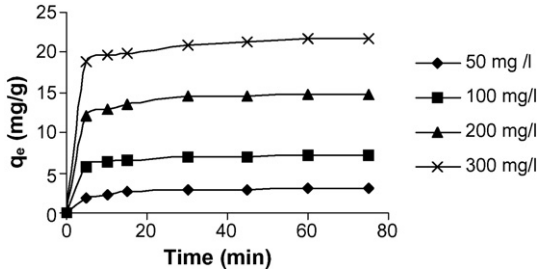

Fig. 2. Effect of time for the adsorption of *m*-cresol onto RHAC-C900 carbon (pH 2.5, temperature 293 K).

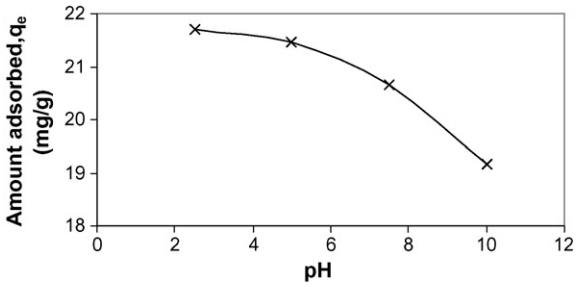

Fig. 3. Effect of uptake of *m*-cresol onto RHAC-C900 carbon at different pH (temperature 293 K; concentration 300 mg/l).

respect to time are single smooth and continuous leading to saturation.

3.3. Effect of pH

The solution pH is one of the key factor that controls the adsorption process on carbon materials because it controls the electrostatic interactions between the adsorbent and the adsorbate. The uptake of the *m*-cresol by the RHAC-C900 decreased with increasing pH as shown in Fig. 3. The adsorption was maximum at pH 2.5 and decreased thereafter. Hence, the optimum pH value was determined as 2.5. At low pH 2.5 (<pH_{ZPC}), the carbon surface is positively charged and as there is no electrostatic repulsion between the unionized *m*-cresol species and the positively charged surface, thus adsorption is higher. Since at pH 10 (>pH_{PZC}) the carbon surface is negatively charged resulting in reduced adsorption due to electrostatic repulsion between the negative surface charge of activated carbon and the *m*-cresol species. Despite this electrostatic repulsion at higher pH, a significant adsorption takes place indicating that chemisorption might have involved in the process [17]. The surface functional groups present in the carbon C900 may also enhance the adsorption of *m*-cresol.

3.4. Effect of concentration

When initial cresol concentration was increased from 50 to 300 mg/l, the loading capacity increased from 3.03 to 21.70 mg/g of activated carbon. It is also evident from Fig. 2 that most adsorption is completed within the early time period of ∼15 min at all the concentrations. Initially the number of active sites available is higher and the driving force for the mass transfer is greater. Therefore, the adsorbate reaches the adsorption site with ease. As time progresses the number of available free active sites become less and the adsorbate molecules are collected at the surface thus impeding the movement of the adsorbate leading to nonlinear adsorption. This can be accounted for the decrease in adsorption rate after 15 min. Thus, the initial concentration provides an important driving force to overcome all mass transfer resistances of the *m*-cresol between the aqueous and solid phases. Hence, a higher concentration of *m*-cresol solution enhances the sorption process and is evidenced from the plot of rate of adsorption with increasing cresol concentration as shown in Fig. 4. The increase of loading capacities of the sorbents with increasing *m*-cresol concentration may also be due to

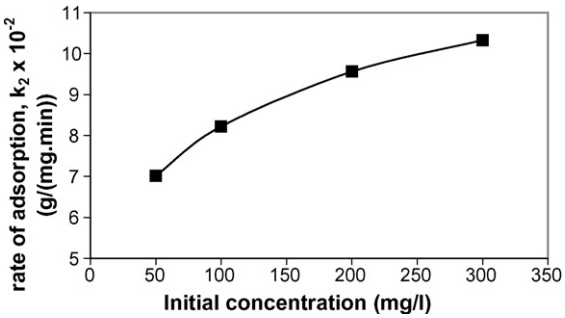

Fig. 4. Effect of pseudo-second-order adsorption rate constant of *m*-cresol on C900 as a function of adsorbate concentration (condition: pH 2.5 and temperature 293 K).

higher π–π dispersion interactions between the aromatic ring of *m*-cresol and the graphene layers of the activated carbon, C900 [18].

3.5. Effect of temperature

Temperature has vital effect on adsorption process as it can increase or decrease the amount of adsorption. The plot of adsorption capacity as a function of temperature is shown in Fig. 5. The equilibrium uptake of *m*-cresol molecules by C900 decreased with increase in temperature from 293 to 323 K indicating that physical adsorption takes place. With increase in temperature from 293 to 323 K The adsorption of *m*-cresol at pH 2.5, 5, 7.5 and 10 was found to decrease from 93.96 to 87.10%, 92.91 to 80.09%, 89.41 to 72.11% and 82.87 to 64.55%, respectively, at a concentration of 300 mg/l. This suggests that the process is exothermic indicating that lower temperature is more favourable for the adsorption of cresol. At higher temperatures between 313 and 323 K, the adsorption was low due to the decrease in physical forces responsible for adsorption or due to the decrease in the intraparticle diffusion rate of cresol into the pores or could also be due to the enhancement of thermal energies of C900, resulting in the weakening of the attractive force between C900 and *m*-cresol preventing to retain the adsorbed molecules at the active sites [19].

3.6. Equilibrium modeling

3.6.1. Langmuir isotherm

The Langmuir equation [20] is applicable to homogeneous sorption where the sorption of each sorbate molecule on to the

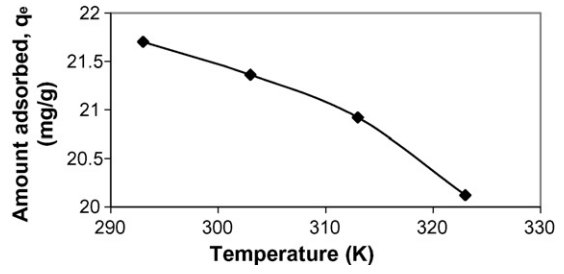

Fig. 5. Uptake of *m*-cresol on the RHAC-C900 carbon at different temperatures (pH 2.5; concentration 300 mg/l).

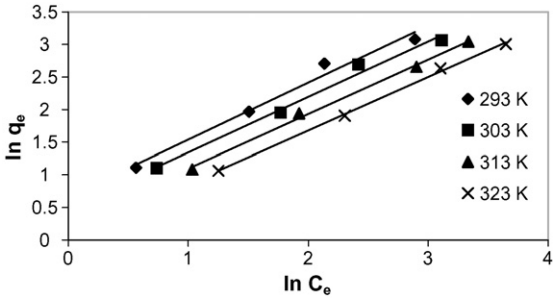

Fig. 6. Freundlich adsorption isotherm of *m*-cresol on to RHAC-C900 at pH 2.5.

surface has equal sorption activation energy and is represented by the linearised expression:

$$\frac{C_e}{q_e} = \frac{1}{K_L} + \frac{a_L}{K_L} C_e \quad (2)$$

where q_e is the solid phase sorbate concentration at equilibrium (mg/g), K_L the Langmuir isotherm constant (l/g), and a_L is the Langmuir isotherm constant (l/mg).

The Langmuir constants were evaluated from the slope a_L/K_L and intercept $1/K_L$ of the linear plot of C_e/q_e versus C_e, using Eq. (2), where K_L/a_L gives the theoretical monolayer saturation capacity Q_0. The isotherms at all range of studied pH and temperatures were not found to be linear over the whole range of concentrations as evidenced from the values of correlation coefficients (R^2) obtained in the range 0.75–0.90. This implies that the adsorption equilibrium data do not exactly fit the Langmuir model of adsorption.

3.6.2. Freundlich isotherm

The most important multisite adsorption isotherm for heterogeneous surfaces is the Freundlich adsorption isotherm [21] that is characterized by the heterogeneity factor $1/n$ and is represented by the linearised equation:

$$\ln q_e = \ln K_F + \frac{1}{n} \ln C_e \quad (3)$$

where q_e is the solid phase concentration in equilibrium (mg/g), C_e the liquid phase sorbate concentration at equilibrium (mg/l), K_F the Freundlich constant (l/g), and $1/n$ is the heterogeneity factor.

The plot of $\ln q_e$ versus $\ln C_e$ enables the constants K_F and exponent $1/n$ to be determined. The plots are shown in Fig. 6. The Freundlich isotherm parameters and the linear regression coefficients are shown in Table 3. Examination of the data showed that the Freundlich model was able to fit the adsorption data for all of the studied pH and temperature range whereby, the correlation coefficients R^2 in the range 0.97–0.99 were obtained. The amount adsorbed on to the material is the summation of adsorption on all sites. Thus, it is inferred that *m*-cresol adsorption satisfying Freundlich isotherm describes reversible adsorption and the occurrence for multilayer adsorption but not restricted to the formation of monolayer. The higher uptake of *m*-cresol at lower pH and temperature can be accounted for more activity of surface groups present in C900 as evidenced from the FTIR spectrum. This model suggests that *m*-cresol adsorption mainly occur in an interval of adsorption energies as it is assumed. The highest K_F and $1/n$ values were found as 1.94 and 0.87, respectively, at pH 2.5 and temperature 293 K. Similarly the lowest value of 0.33 and 0.81 of K_F and $1/n$ values were obtained at pH 10 and temperature 323 K. Table 3 also indicates that n is greater than unity, indicating that *m*-cresol molecules are favourably adsorbed onto activated carbon at all temperatures. The values of K_F gradually decrease with rise in temperature and pH. These findings validate that adsorption is favourable at low temperature and at low pH.

3.6.3. Dubinin–Radushkevich (D–R) equation

The D–R isotherm is more common than the Langmuir isotherm because it does not assume a homogenous surface or constant sorption potential [22]. The theory of volume filling of micropores, expressed via the D–R equation is based on the concept of Polanyi. This theory assumes that there is a variable adsorption potential where the free energy of adsorption is related to the degree of pore filling. The D–R equation is given as

$$q_e = q_{DR} \exp(-\beta \varepsilon^2) \quad (4)$$

where q_e is the amount of *m*-cresol adsorbed at equilibrium, β a constant related to the adsorption energy, q_{DR} the maximum adsorption capacity in the micropores, and ε is the Polanyi potential.

The Polanyi adsorption potential ε for the liquid phase is defined by

$$\varepsilon = RT \ln \left(\frac{C_s}{C_e} \right) \quad (5)$$

where R is the gas constant, T the temperature and C_s is the solubility of the solute.

Table 3
Freundlich sorption isotherm constants for the adsorption of *m*-cresol onto RHAC-C900

pH	Temperature											
	293 K			303 K			313 K			323 K		
	K_F ((mg/g)(mg/l)^n)	$1/n$	R^2	K_F ((mg/g)(mg/l)^n)	$1/n$	R^2	K_F ((mg/g)(mg/l)^n)	$1/n$	R^2	K_F ((mg/g)(mg/l)^n)	$1/n$	R^2
2.5	1.94	0.87	0.97	1.63	0.85	0.98	1.29	0.84	0.99	1.03	0.82	0.99
5	1.70	0.86	0.97	1.24	0.83	0.99	1.01	0.83	0.99	0.61	0.82	0.99
7.5	1.16	0.83	0.99	0.95	0.84	0.98	0.88	0.83	0.99	0.39	0.86	0.98
10	0.76	0.83	0.99	0.62	0.81	0.99	0.53	0.812	0.99	0.33	0.81	0.99

Table 4
Parameters for the Dubinin–Radushkevich (D–R) adsorption isotherms for the adsorption of *m*-cresol onto RHAC-C900

pH	Temperature															
	293 K				303 K				313 K				323 K			
	q_{DR} (mmol/g)	V_{DR} (cm^3/g)	E (kJ/mol)	R^2	q_{DR} (mmol/g)	V_{DR} (cm^3/g)	E (kJ/mol)	R^2	q_{DR} (mmol/g)	V_{DR} (cm^3/g)	E (kJ/mol)	R^2	q_{DR} (mmol/g)	V_{DR} (cm^3/g)	E (kJ/mol)	R^2
2.5	2.27	0.23	11.26	0.98	1.82	0.19	11.47	0.98	1.51	0.15	11.76	0.99	1.22	0.12	12.09	0.98
5	1.94	0.20	11.08	0.97	1.46	0.15	11.38	0.99	1.33	0.13	11.56	0.99	0.09	0.10	11.67	0.98
7.5	1.36	0.14	11.01	0.98	1.26	0.13	10.37	0.99	1.28	0.13	11.41	0.99	0.08	0.09	11.41	0.99
10	1.16	0.12	10.60	0.99	0.83	0.09	10.07	0.97	0.83	0.08	11.26	0.98	0.05	0.06	11.13	0.96

The characteristic adsorption energy E in the micropores is given by the relation:

$$E = \frac{1}{\beta^{1/2}} \tag{6}$$

The D-R equation (4) can be linearised as

$$\ln q_e = \ln q_{DR} - \left(\frac{RT}{E}\right)^2 \left(\ln\left(\frac{C_s}{C_e}\right)\right)^2 \tag{7}$$

Thus, in brief the D–R equation results in an estimation of maximum adsorption capacity, q_{DR}; the total micropore volume, V_{DR} of the adsorbent as well as free energy value E unique to the adsorbent adsorbate system.

The plot of $\ln q_e$ versus $(\ln (C_s/C_e))^2$ shown in Fig. 7 enables to determine the parameters of the D–R equation for the adsorption of *m*-cresol and are shown in Table 4. The correlation coefficients are also shown. According to the above mentioned D–R hypothesis, this model could exactly fit the isotherm data well because the correlation coefficient were in the range 0.97–0.99 and thus this model describes the adsorption process as a pore filling effect and does not assume a homogenous surface or constant potential. The micropore volume, V_{DR} and the adsorption energy, E varied with temperature. The total micropore volume accessible to *m*-cresol molecules gradually decreased with increase in pH and temperature. The maximum amount of micropore volume filled was 0.23 cm^3/g at a reaction condition of pH 2.5 and 293 K while the minimum filling of 0.06 cm^3/g occurred at pH 10 and 323 K. The decrease in physical forces responsible for adsorption could be the reason for such a low filling at high temperature and pH. As for the mean free energy that is determined from the D–R equation, the value of E was also found to be decreasing with increase in pH demonstrating that the *m*-cresol molecules do not get easy access into the micropores as well. Moreover, at lower temperature and pH the value of V_{DR} derived from the liquid phase adsorption, 0.23 cm^3/g was found to be similar to the micropore volume determined by D–R equation using N_2 adsorption, 0.23 cm^3/g (value not shown in Table 2). This indicates that the micropores are fully utilized in the liquid phase adsorption of *m*-cresol at such low conditions.

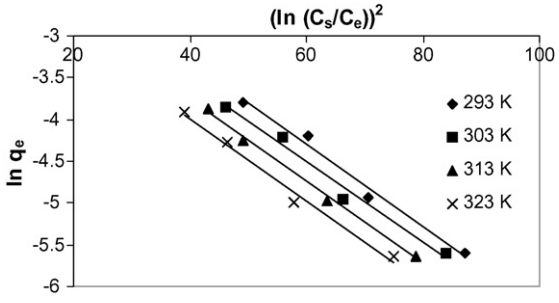

Fig. 7. D–R adsorption isotherm of *m*-cresol on to RHAC-C900 at pH 2.5.

3.7. Validity of kinetic modeling

In order to investigate the adsorption process of *m*-cresol onto micro/mesoporous carbon, C900 the frequently used kinetic models such as the linearised form of pseudo-first-order, pseudo-second-order and intraparticle diffusion models given in Eqs. (8) and (9), respectively, were used to determine the mechanism of adsorption process. The equations are represented as [23,24]:

$$\ln (q_e - q_t) = \ln q_e - k_1 t \tag{8}$$

$$\frac{t}{q_t} = \frac{1}{k_2 q_e^2} + \frac{1}{q_e} t \tag{9}$$

where q_e and q_t is the amount of *m*-cresol adsorbed (mg/g) at equilibrium and at time (min), k_1 the first-order equilibrium rate constant (min^{-1}) and k_2 is the pseudo-second-order rate constant.

The validity of the order of adsorption process were based on the two criteria, first based on the regression coefficient and secondly based on the calculated q_e values. The calculated q_e were obtained from the constant term of Eq. (8) and from the slope of Eq. (9) for the first- and second-order equations, respectively. The first-order rate constants k_1 were evaluated from the plots of $\ln (q_e - q_t)$ versus t. The correlation coefficients obtained were in the range 0.86–0.96 and the calculated q_e values obtained from the first-order kinetic model do not agree with the experimental values as shown in Table 5. This indicates that the adsorption of *m*-cresol onto RHAC-C900 do not follow the first-order kinetic model. The linear plots of t/q_t versus t in Fig. 8 yielded the second-order rate constant k_2. The q_e value calculated from the slope of the equation had a good agreement with the experimental q_e values as seen in Table 5. Moreover, the correlation coefficients for the second-order kinetic model are greater than 0.99. Thus, it is inferred that the adsorption system belong to the second-order kinetic model.

Table 5
Comparison of the first- and second-order rate constants with experimental and calculated q_e values for *m*-cresol at pH 2.5

Parameter		First-order kinetic model				Second-order kinetic model		
Concentration (mg/l)	Temperature (K)	q_e (mg/g) (experimental)	q_e (mg/g) (calculated)	k_1 ($\times 10^{-2}$ min^{-1})	R^2	k_2 ($\times 10^{-2}$ g/(mg min))	q_e (mg/g) (calculated)	R^2
100	293	7.16	1.59	6.49	0.94	8.22	7.29	1.00
	303	7.03	1.73	7.79	0.96	7.16	6.11	0.99
	313	6.95	3.04	8.36	0.94	6.15	7.20	0.99
	323	6.70	3.88	7.28	0.94	5.26	7.06	0.99
300	293	21.70	5.42	7.42	0.88	10.3	22.07	0.99
	303	21.36	7.97	9.01	0.95	9.02	21.88	0.99
	313	20.92	5.37	7.93	0.92	8.24	21.45	0.99
	323	20.12	1.79	8.02	0.95	6.89	20.70	0.99

Eqs. (8) and (9) cannot identify the diffusion mechanism. Therefore, the intraparticle diffusion model is thus tested which refers to the theory proposed by Weber and Morris [25]. The rate of intraparticle diffusion can be obtained from the linearised curve $q_t = k_d\sqrt{t}$. Such type of plots may present a multi-linearity implying the two or more steps occur [26]. The first sharper portion is the external surface adsorption stage. The second portion is the gradual adsorption stage, where the intraparticle diffusion is rate limited. The third portion is final equilibrium stage where the intraparticle diffusion starts to slow down due to extremely low soluble concentration in the solution. A good correlation of rate data in this model can justify the mechanism. The slope of the linear portion of the plot between q_t versus $\sqrt{t}$ has been defined as a rate parameter (k_d) which characterizes the rate of adsorption in the region where pore diffusion is rate limiting. The intercept of the plot (δ) on the other hand signifies the extent of boundary layer effect, i.e. the larger the intercept the greater is the contribution of the surface adsorption in the rate-limiting step [26].

The plots in Fig. 9, q_t versus $\sqrt{t}$ suggest that adsorption consisting of both surface adsorption and the intraparticle transport within the pores of the carbon. The initial curved portion of the plot indicates boundary layer effect, i.e. surface adsorption. The intercept of the plot signifying the boundary layer effect and the slope signifying the rate parameter is listed in Table 6. In the present study two different regions of rates of uptake were observed. The rate of uptake is initially slightly faster and then slows down. It is likely that initially the adsorbate is transported to the mesopore and then it is slowly diffused into the micropores. Thus, all these suggest that in the adsorption of *m*-cresol over the carbon C900, the pore diffusion phenomenon plays a significant role.

3.8. Calculation of thermodynamic parameters (ΔG°, ΔH°, ΔS°)

The change in standard free energy ΔG°, the enthalpy ΔH° and the entropy, ΔS° of adsorption of *m*-cresol by RHAC-C900 were calculated by the following thermodynamic equations [27]:

$$\Delta G^\circ = -RT \ln K_c \tag{10}$$

and

$$K_c = \frac{C_{Ae}}{C_e} \tag{11}$$

where R is the gas constant, T the temperature (K), K_c the equilibrium constant, C_{Ae} the equilibrium concentration of solute on the adsorbent and C_e is the equilibrium concentration in the solution.

The values of ΔH° and ΔS° were calculated from the slope and intercept respectively of the linear Van't Hoff plot [28] as shown in Fig. 10:

$$\ln K_c = \frac{\Delta S^\circ}{R} - \frac{\Delta H^\circ}{RT} \tag{12}$$

where ΔS° and ΔH° are the changes in entropy and enthalpy of the adsorption.

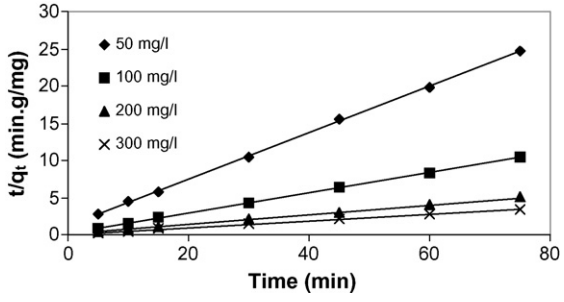

Fig. 8. Plot of second-order kinetic model at different concentration on to C900 (temperature 293 K, pH 2.5).

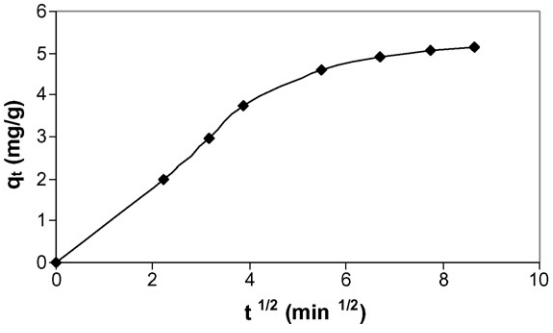

Fig. 9. Plot of Weber and Morris equation for *m*-cresol onto RHAC-C900 (concentration 100 mg/l, temperature 323 K, pH 10).

Table 6
Pore diffusion parameter, k_d and boundary layer effect parameter, δ for the adsorption of *m*-cresol onto activated carbon (pH 2.5)

Concentration (mg/l)	293 K		303 K		313 K		323 K	
	k_d ($\times 10^{-2}$ mg g^{-1} min$^{-1/2}$)	δ (mg/g)	k_d ($\times 10^{-2}$ mg g^{-1} min$^{-1/2}$)	δ (mg/g)	k_d ($\times 10^{-2}$ mg g^{-1} min$^{-1/2}$)	δ (mg/g)	k_d ($\times 10^{-2}$ mg g^{-1} min$^{-1/2}$)	δ (mg/g)
50	6.02	2.60	5.63	2.24	5.08	2.31	4.10	2.08
100	12.0	6.19	9.46	6.41	8.05	5.97	7.45	5.36
200	34.5	12.32	32.57	12.24	25.56	12.1	21.51	11.20
300	44.3	18.14	41.17	17.39	40.41	17.13	36.09	15.66

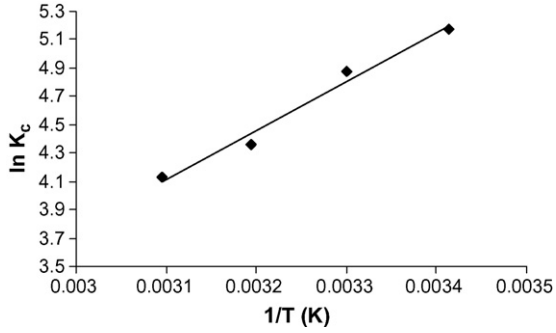

Fig. 10. Van't Hoff plot for the adsorption of *m*-cresol onto RHAC activated carbon.

The values of ΔG°, ΔH°, ΔS° are listed in Table 7. The negative values of ΔG° confirms the feasibility of the adsorption process and also indicate that the adsorption of *m*-cresol on activated carbon occurs via a spontaneous process. The decrease in the value of $-\Delta G^\circ$ with increasing temperature indicate that the sorption of cresol on to the activated carbon is less favourable at higher temperatures. The enthalpy change of adsorption was found to be negative. This negative value of enthalpy change confirms the exothermic nature of the adsorption of cresol onto C900. The low enthalpy value of $\Delta H^\circ < 20$ kJ/mol for the present system confirms that physisorption is involved in the adsorption process of *m*-cresol onto C900. The estimated value of ΔH° for the present system was in the range −23.46 kJ/mol to −25.40 kJ/mol. Since *m*-cresol adsorbed on C900 form stronger bonding at pH 2.5 than at pH 10, the enthalpy of adsorption is comparatively high at the lower pH range. The heat of physical adsorption decreasing at pH 10 clearly indicate that the high energy centers are not properly occupied as a result of weak attractive forces between the adsorbate and the adsorbent. The negative value of ΔS° suggest a decrease in degree of freedom of the adsorbed species. The increase in the magnitude of entropy ($-\Delta S^\circ$) from 19.44 to 35.87 with increase in pH from 2.5 to 10 as seen in Table 7, may be due to the decrease in the randomness at the solid–solution interface during the adsorption process as a result of decrease in the distribution of rotational and translational energy among the molecules.

Table 7
Thermodynamic parameters for the sorption of *m*-cresol onto C900 carbon

pH	Temperature (K)	ΔH° (kJ/mol)	ΔG° (kJ/mol)	ΔS° (J/(mol K))
2.5	293	−23.46	−17.70	−19.44
	303		−17.65	
	313		−17.40	
	323		−17.12	
10	293	−25.40	−15.57	−35.87
	303		−14.80	
	313		−14.49	
	323		−13.54	

3.9. Influence of mesopores

It is commonly known that the major adsorption occurs in the micropores while weaker adsorption occurs in the mesopores. Generally adsorption process would proceed through a sequence of diffusion steps from the bulk phase into the mesopores and then to the micropores. During this diffusion process pore blockage may occur due to the aggregation of adsorbate molecules or due to the smaller cross sectional area of some micropores [29]. Hence, if the diffusion path is longer then there would be a possibility of pore blocking leading to reduced adsorption. Therefore, in the RHAC-C900 used in the present work, the presence of considerable mesopores volume (69.23%) behaves as an entrance for the movement of cresol molecules from the bulk phase to the inner micropores without any hindrance. Thus, during the diffusion process the presence of mesopore is of great advantage enabling easy access to the micropores not only for accelerating the diffusion into micropores but also in increasing the equilibrium coverage of micropore surface. The complete micropore volume filled by the *m*-cresol molecule is a good evidence for this. It is observed that the total micropore volume estimated using the D–R equation from the N_2 adsorption analysis (not shown in the Table 2) and *m*-cresol adsorption on to C900 carbon is 0.23 and 0.23 cm^3/g, respectively, confirming the utility of micropores in RHAC. The higher adsorption capacity of the carbon can thus be explained by the fact that the carbon containing considerable mesopore volume leading to the shortening of the diffusion path of micropores for *m*-cresol to get easy access to the carbon interior [30].

3.10. Mechanism of the adsorption process

The adsorption of organics on activated carbon is dependent to a large extent on the chemistry of carbon surface. The heterogeneous surface of activated carbon such as the carbon basal planes and the surface groups especially oxygen containing groups play a dominant role in the adsorption process. During the adsorption process the *m*-cresol molecules can be adsorbed

in a planar position on the basal planes that are held by the attractive forces operating over the entire aromatic ring or the *m*-cresol molecules at higher adsorbate concentration may get packed more tightly on the surface and thought to be adsorbed in vertical orientation, i.e. end on position, resulting in the interaction among adsorbed *m*-cresol molecules [29]. Therefore, the mechanism can be explained on the basis of influence of oxygen groups on the dispersive/repulsive interactions between the basal planes and the adsorbed molecules [31].

The physical adsorption of aromatic compounds onto activated carbon takes place mainly through dispersive interactions between the aromatic molecules and the carbon planes. These dispersive interactions are basically in the form of Van der Waals interactions [32]. The oxygen groups present at the surface of the carbon removes and localize the electrons from the π-electron system of the carbon basal planes, creating positive holes in the conductive π-band of the graphitic planes. The functional group (–OH) attached to the aromatic adsorbate is an activating group [33]. The activating group acts as electron donors which create a partially negative aromatic ring by drifting the electrons towards the ring, thus making the aromatic ring of cresol molecule to develop dipoles. The negative end of the dipole interacts with positive charged active sites of the carbon basal plane. The positive end of the cresol molecule induces the neighboring molecules to undergo polarization leading to dipolar interactions between the successive molecules. This ultimately resulted with development of bonding in the direction perpendicular to the *X* plane of the carbon surface. In addition it is also proposed that aromatic compounds with a functional group is capable of forming H-bonding with neighboring cresol molecules lateral to the plane of the carbon surface. Thus, the mechanism suggests that the multilayer adsorption takes place both in the perpendicular and lateral directions through dipole–dipole interaction and H-bonding, respectively.

4. Conclusion

The investigations are quite useful in developing an appropriate technology for wastewater treatment using the carbon C900. The maximum adsorption occurred at pH 2.5 and temperature 293 K. Freundlich and the Dubinin–Radushkevich model was demonstrated to provide the best correlation for the sorption of *m*-cresol onto RHAC–C900 than the Langmuir model. The models suggested that *m*-cresol adsorption follows physical adsorption. The physical adsorption occurs as a result of interactions between the aromatic part of cresol and the carbon's basal planes. The experimental data reveal that within the studied concentration range, the micropore filling is completed followed by adsorption occurring on the mesopore surface by multilayer adsorption. The adsorption kinetics of the systems studied was found to be diffusion controlled. A possible mechanism of adsorption is also suggested. The sorption process is found to be exothermic in nature with a negative value of entropy, ΔS suggesting a decrease in degree of freedom of the adsorbed species. The negative value of Gibbs free energy, ΔG indicates that the adsorption occurs via a spontaneous process. On the basis of the data, it can be concluded that abundant availability of rice husk of little utility can be carbonized and can have wide potential as a cheap and adsorbent.

Acknowledgement

The authors highly thank the Council of scientific and industrial research (CSIR), India by providing financial assistance to carry out this work.

References

[1] D.L. Venter, I. Nieuwoudt, Separation of *m*-cresol from natural oils with liquid–liquid extraction, Ind. Eng. Chem. Res. 37 (1998) 4099–4106.
[2] A. Kumar, S. Kumar, S. Kumar, Adsorption of resorcinol and catechol on granular activated carbon: equilibrium and kinetics, Carbon 41 (2003) 3015–3025.
[3] G. Dursun, H. Cicek, A.Y. Dursun, Adsorption of phenol from aqueous solution by using carbonized beet pulp, J. Hazard. Mater. B 125 (2005) 175–182.
[4] R.S. Juang, F.C. Wu, R.L. Tseng, Mechanism of adsorption of dyes and phenols from water using activated carbons prepared from plum kernels, J. Colloid Interf. Sci. 227 (2000) 437–444.
[5] A. Imagawa, R. Seto, Y. Nagaosa, Adsorption of chlorinated hydrocarbons from air and aqueous solutions by carbonized rice husk, Carbon 38 (2000) 628–630.
[6] Y. Guo, J. Qui, S. Yang, K. Yu, Z. Wang, H. Xu, Adsorption of Cr(VI) on micro- and mesoporous rice husk based active carbon, Mater. Chem. Phys. 78 (2003) 132–137.
[7] P.K. Malik, Use of activated carbons prepared from saw dust and rice husk for adsorption of dyes: a case study of Acid Yellow 36, Dyes Pigments 56 (2003) 239–249.
[8] Y. Guo, J. Qui, S. Yang, K. Yu, Z. Wang, H. Xu, Adsorption of malachite green on micro- and mesoporous rice husk based active carbon, Dyes Pigments 56 (2003) 219–229.
[9] Y. Guo, J.H. Zang, N. Tao, Y. Liu, J. Qi, Z. Wang, H. Xu, Adsorption of malachite green on micro- and mesoporous rice husk based active carbon, Mater. Chem. Phys. 82 (2003) 107–115.
[10] J. Qui, Z. Li, Y. Guo, H. Xu, Adsorption of phenolic compounds on micro- and mesoporous rice husk based active carbon, Mater. Chem. Phys. 87 (2004) 96–101.
[11] Y. Guo, J. Zhao, H. Zhang, J. Qui, S. Yang, Z. Wang, H. Xu, Use of rice husk based porous carbon for adsorption of rhodamine B from aqueous solutions, Dyes Pigments 66 (2005) 123–128.
[12] N.R. Bishnoi, M. Bajaj, N. Sharma, A. Gupta, Adsorption of Cr(VI) on rice husk carbon and activated alumina, Bioresour. Technol. 91 (2004) 305–307.
[13] I.A. Rahman, B. Saad, S. Shaidan, E.S.S. Rizal, Adsorption characteristics of malachite green on activated carbon derived from rice husks produced by chemical thermal process, Bioresour. Technol. 96 (2005) 1578–1583.
[14] M. Akhtar, M.I. Bhanger, S. Iqbal, S.M. Hasany, Sorption potential of rice husk for the removal of 2,4-dichlorophenol from aqueous solution: kinetic and thermodynamic investigations, J. Hazard. Mater. 128 (2006) 44–52.
[15] L.J. Kennedy, J.J. Vijaya, G. Sekaran, Effect of two stage process on the preparation and characterization of porous carbon composite from rice husk by phosphoric acid activation, Ind. Eng. Chem. Res. 43 (2004) 1832–1838.
[16] M.S. Solum, R.J. Pugmire, M. Jagtoyen, F. Derbyshire, Evolution of carbon structure in chemically activated wood, Carbon 33 (1995) 1247–1254.
[17] C. Namasivayam, D. Kavitha, Adsorptive removal of 2-chloropjenol by low cost coir pith carbon, J. Hazard. Mater. B98 (2003) 257–274.
[18] C. Moreno-Castilla, Adsorption of organic molecules from aqueous solutions of organic materials, Carbon 42 (2004) 83–94.
[19] D.N. Jadhav, A.K. Vanjara, Removal of phenol from wastewater using sawdust, polymerized saw dust and saw dust carbon, Indian J. Chem. Tech. 11 (2004) 35–41.
[20] I. Langmuir, The adsorption of gases on plane surfaces of glass, mica and platinum, J. Am. Chem. Soc. 40 (1918) 1361–1403.

[21] H.M.F. Freundlich, Over the adsorption in solution, Z. Phys. Chem. 57 (1906) 57–63.
[22] S.B. Stuart, Adsorption from dilute, binary aqueous solutions, J. Colloid Interf. Sci. 158 (1993) 64–70.
[23] Z. Aksu, Y.A. Julide, Comparative adsorption/biosorption study of monochlorinated phenols onto various sorbents, Waste Manage. 2 (2000) 695–699.
[24] F.A. Banat, S. Al-Asheh, L. Al-Makhadmeh, Utilization of raw and activated date pits for the removal of phenol from aqueous solutions, Chem. Eng. Technol. 27 (2004) 80–86.
[25] W.J. Weber, J.C. Morris, Proc. Int. Conf. on Water Poll. Symp., vol. 2, Pergamon Press, Oxford, 1962, pp. 231–266.
[26] S. Mitali, A.P. Kumar, B. Bhaskar, Modeling the adsorption kinetics of some priority organic pollutants in water from diffusion and activated energy parameters, J. Colloid Interf. Sci. 206 (2003) 28–32.
[27] K. Nasir, A. Shujaat, T. Aqidat, A. Jamil, Immobilization of arsenic on rice husk, Adsorp. Sci. Technol. 16 (1997) 655–666.
[28] W.J. Min, K.H. Ahn, Y. Lee, K.P. Kim, J.S. Rhee, J.T. Park, K.J. Paeng, Adsorption characteristics of phenol and chlorophenols on granular activated carbon, Microchem. J. 70 (2001) 123–131.
[29] C.T. Hsieh, Influence of mesopore volume and adsorbate size on adsorption capacities of activated carbon in aqueous solution, Carbon 38 (2000) 863–869.
[30] H. Teng, C.T. Hsieh, Influence of surface characteristics on liquid phase adsorption of phenol by activated carbons prepared from bituminous coal, Ind. Eng. Chem. Res. 37 (1998) 3618–3622.
[31] M. Franz, H.A. Arafat, G.P. Neville, Effect of chemical surface heterogeneity on the adsorption on activated carbon, Carbon (2000) 1807–1819.
[32] Y. Leon, C. Leon, L. Radovic, Interfacial chemistry and electrochemistry of carbon surfaces, in: P.A. Thrower (Ed.), Chemistry and Physics of Carbon, Marcel Dekker, 1994, pp. 213–310.
[33] R.T. Morrison, R.N. Boyd, Organic Chemistry, 6th ed., Prentice Hall, India, 1999.